A Case Study on Influence of Utilizing Hill-type Muscles on Mechanical Efficiency of Biped Running Gait

B. Dadashzadeh[1*], A. Allahverdizadeh[1], M. Esmaeili[1], H. Fekrmandi[2]

The presence of compliant elements in biped running mechanisms generates a smoother motion and decreases impact forces. Biological creatures that have a complicated actuation system with parallel and series elastic elements in their muscles demonstrate very efficient and robust bipedal gaits. The main difficulty of implementing these systems is duplicating their complicated dynamics and control. This paper studies the effects of an actuation system, including Hill-type muscles on the running efficiency of a kneed biped robot model with point feet. In this research, we implement arbitrary trajectories compatible with the initial condition of the robot, and we calculate the necessary muscle forces using an analytical inverse dynamics model. To verify the results, we execute the direct dynamics of the robot with the calculated control inputs to generate the robot's trajectory. Finally, we calculate the contractile element force of the muscles and its cost of transport, and we investigate the effects of the muscles' elements on reducing or increasing the cost of transport of the gait and maximum actuating forces.

Keywords: Biped Running, Gait Planning, Hill-type Muscle, Cost of Transport

1. Introduction

Despite numerous research on planning and controlling bipedal running, there is still no biped robot capable of running as efficiently as animals. In this area, the main difference between robots and animals is that, in robots, muscles are replaced with electric or pneumatic motors. Developing actuators that operate with a dependency on muscle structure can be a solution for future robotic efficiency. In this research, we consider Hill-type muscles instead of rotational motors as actuators of a biped robot model. Additionally, we plan periodic running gaits including a stance phase, take-off event, flight phase, and touch-down event.

By investigating muscle structure, Hill [1] described its mechanical model elements as follows: one contractile

---

[1] Department of Mechatronics Engineering, Faculty of Mechanical Engineering, University of Tabriz, Tabriz, Iran, Corresponding author E-mail: b.dadashzadeh@tabrizu.ac.ir

[2] Department of Mechanical Engineering, South Dakota School of Mines & Technology, Rapid City, USA

element; a series elastic element; and a parallel elastic element. This model has been used by biomechanics researchers as a base model for muscles. Lichtwark *et al.* [2] used ultrasonic sensors to detect length variations of muscle elements during walking and running. Iida *et al.* [3] proposed bi-articular springs on the thigh and shin, instead of muscles for a robot with minimal hip actuation, which could generate walking and a special running gait in experiments.

Pneumatic artificial muscles have been developed as a mechanical realization of muscles. However, they have some drawbacks; pneumatic muscles have small movement strides, and it is difficult to supply compressed air for a biped robot. Hosoda *et al.* [4] used antagonistic pneumatic actuators to generate biped walking and running gaits and showed that pneumatic actuators have good characteristics to generate human-like motion. Niiyama [5] developed a biped robot, named Athlete, with pneumatic artificial muscles that could run eight steps with a forward speed of 3 m/s.

The Spring Loaded Inverted Pendulum (SLIP) model with a spring and point mass has been proven as a basic and efficient model for biped walking and running [6]. Also, the Point Mass Biped (PMB) model consisting of a point mass and prismatic force actuator can generate biped walking and running gaits by minimizing mechanical work costs [7], as well as smoother force profiles by minimizing a hybrid cost function including mechanical work, leg force, and its derivatives [8]. PMB model has proven to be a more general model than a SLIP model, capable of generating arbitrary trajectories for bipedal running with single-hump and double-hump ground reaction force (GRF) profiles [9]. Minimal robots have been fabricated based on these models. For example, monopod II [13] has an energy expenditure closer to these basic models than real robots like HRP-2L [14]. However, it has very limited motion capabilities. To generate efficient biped running gaits, the gait model of the main biped robot can be optimized, or a minimal optimal template can be tracked by the main robot. Guo *et al.* [10] proposed a nonlinear optimization algorithm to generate optimal biped running gaits with different velocities on level ground and stairs. Also, the SLIP model has been used as a template to control the running of real biped robots using HZD [11] and force control [12].

Since biological actuation systems perform better than mechanical robots, this work simulates and investigates the benefits or drawbacks of the Hill-type muscle in bipedal running by studying the effects of muscle parameters on running efficiency. The existence of a spring series with the motor isolates external impulsive forces from the motor but makes it difficult to control [18], [12]. Where compliance exists in parallel to the motor, spring torque can reduce the required torque of the motor [15], [16]. With a Hill-type muscle, the benefits or drawbacks of both cases may influence the system. Also, a PMB model instead of a SLIP model is used as a template for the multibody biped model.

2. Muscled Biped Robot Model

2.1. *Multibody Robot Model*

This paper considers a 5-link planar biped model with point feet for dynamic modeling and gait planning, as shown in Fig. 1. Thigh and shin links have mass and moment of inertia that are actuated by Hill-type muscles. The torso angle is assumed to be locked at a vertical orientation ($\theta_5 = 0$). All of the links have the length of $0.5 \ m$. To simplify

the system and build an efficient robotic architecture similar to musculoskeletal systems, a single, tensional-compressive Hill-type muscle is considered for each joint instead of biarticular tensional muscles. This is because a robotic actuator can exert both tensional and compressive forces whereas a biological muscle can exert only tensional force. To enable the muscles to exert torque to links, small and massless bone extensions with equal lengths, $L_6, L_7, L_8 = L_{ex}$, are attached rigidly to thigh 1, the torso, and thigh 2, respectively, with fixed angles. The fixed angles are assumed to be $\theta_6 = \theta_8 = \theta_{ex,knee}$ and $\theta_7 = \theta_{ex,hip}$. Lengths and angles of these extensions will be considered as parameters in gait design. The mass of the shin is 2 kg, the thigh is 2 kg, and the torso is 58 kg.

The running gait consists of a stance phase, take-off event, flight phase, and touch-down event, and their dynamic models are needed for gait planning and simulations.
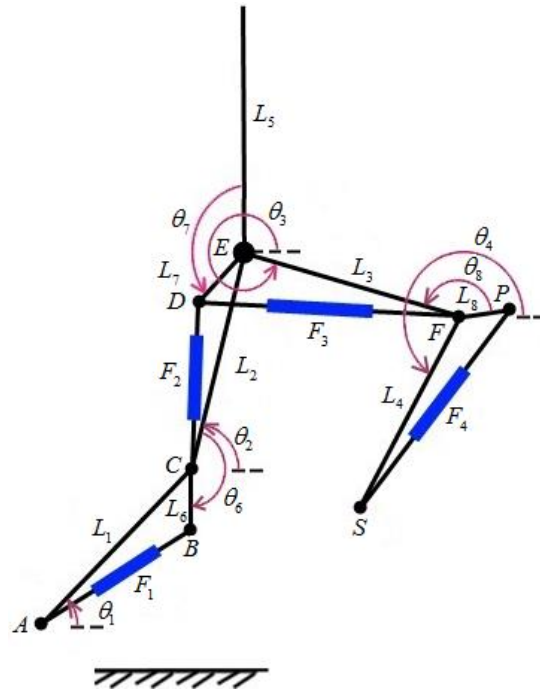
Fig 1. The 5-link biped model with muscle actuation

In the stance phase, point A is pivoted to the ground according to Fig. 1. The robot has 4 DOF[3] with the generalized coordinates of $q_s = [\theta_1, \theta_2, \theta_3, \theta_4]^T$. Input vector $u = [F_1, F_2, F_3, F_4]^T$ consists of muscle output forces. The Lagrange equation is used to obtain the dynamic model of the system.

$$\frac{d}{dt}\frac{\partial L}{\partial \dot{q}} - \frac{\partial L}{\partial q} = Q,$$

---

[3] Degree of Freedom

in which L is the Lagrangian function that is the subtraction of kinetic and potential energies, and $\boldsymbol{Q}$ is the generalized force vector. The positions of each joint and link's COM[4] are written as a function of generalized coordinates, and their velocities are obtained by symbolic differentiation. The kinetic and potential energies of the system are written as a function of generalized coordinates and their time derivatives. Kinetic energy is the sum of translational and rotational kinetic energies of all the links, and potential energy consists of their gravitational potential energies. The muscles and their bone extensions are assumed to be massless, and, because their output forces are considered in the robot model, they do not contribute to kinetic and potential energy terms. Muscle lengths $\overline{AB}, \overline{CD}, \overline{DF}$, and $\overline{PS}$ are written as a function of generalized coordinates, and the generalized forces are calculated using virtual works as

$$Q_i = F_1 \frac{\partial \overline{AB}}{\partial q_i} + F_2 \frac{\partial \overline{CD}}{\partial q_i} + F_3 \frac{\partial \overline{DF}}{\partial q_i} + F_4 \frac{\partial \overline{PS}}{\partial q_i} \quad , \ i = 1,2,3,4.$$

The dynamic equations of the stance phase are summarized as

$$D_s(\boldsymbol{q}_s).\ddot{\boldsymbol{q}}_s + C_s(\boldsymbol{q}_s, \dot{\boldsymbol{q}}_s) = B_s(\boldsymbol{q}_s).\boldsymbol{u}, \tag{1}$$

in which D_s is 4×4 inertia matrix, C_s is 4×1 Coriolis and gravity matrix, and B_s is 4×4 input matrix.

In the flight phase, the robot undergoes a ballistic trajectory and has 6 DOF. Generalized coordinates of the flight phase are chosen as $\boldsymbol{q}_f = [\theta_1, \theta_2, \theta_3, \theta_4, x_E, y_E]^T$ including link angles and hip position. Similarly, the dynamic model of the flight phase is written as

$$D_f(\boldsymbol{q}_f).\ddot{\boldsymbol{q}}_f + C_f(\boldsymbol{q}_f, \dot{\boldsymbol{q}}_f) = B_f(\boldsymbol{q}_f).\boldsymbol{u}, \tag{2}$$

in which D_f is 6×6 matrix, C_f is 6×1, and B_s is 6×4.

The take-off event is an instantaneous transition from the stance to flight phase and takes place when the vertical component of GRF reaches zero. In this instance, the initial state of the flight phase is captured as

$$\boldsymbol{q}_f^+ = [\boldsymbol{q}_s^-; x_E(\boldsymbol{q}_s^-); y_E(\boldsymbol{q}_s^-)],$$

in which superscript + indicates the moment just after the event and – indicates just before the event.

The touch-down event takes place at the end of the flight phase when the toe-tip position reaches ground. The contact is assumed to be fully plastic with no rebound, after which point S makes an ideal pivot to the ground. The toe of the robot should have a sufficient coefficient of friction with the ground to prevent sliding effects. The touch-down map, which is used to convert pre-touch-down velocities to post-touch-down velocities, is derived using Lagrange's impact equation,

$$D_f(\boldsymbol{q}_f).\left(\dot{\boldsymbol{q}}_f^+ - \dot{\boldsymbol{q}}_f^-\right) = \widehat{\boldsymbol{Q}},$$

and two constraint equations of post-contact foot pivoting to the ground. More details can be found in Ref. [16].

2.2. Muscle Model as the Robot Actuating System

Having the necessary forces of the muscle ends (F) known for the running gait, we use a Hill-type muscle

---

[4] Center of Mass

model to calculate its contractile element force (F_h), as shown in Fig. 2. The only difference between the considered muscle model in this paper and a traditional Hill-type muscle model is that the control input F_h generated by a force actuator can be tensile or compressive. k_1 and c_1 represent a stiffness and damping parallel to the force actuator, corresponding to perimysium, endomysium, epimysium, and sarcolemma mechanical properties in a muscle. k_2 is a series elastic component corresponding to a tendon.

To calculate the muscle actuating force F_h, known as the contractile element force, in terms of muscle external force F, dynamic equations of the muscle components (Fig. 2) are used.

$$F = k_2(x_m - x_a - x_{b,0}) \tag{3}$$

$$F_h = -k_1(x_a - x_{a,0}) - c_1 \dot{x}_a + F \tag{4}$$

The time derivative of Eq. (3) is written as

$$\dot{F} = k_2(\dot{x}_m - \dot{x}_a). \tag{5}$$

From kinematic analysis of the desired gait, muscles lengths x_m and their time derivatives $\dot{x}_m$ are known numerically as a function of time. Also, muscles forces F and their time derivatives $\dot{F}$ are known from inverse dynamics, as mentioned in Sections 3.1 and 3.2. Eqs. (3) to (5) are 3 equations with 3 unknowns, F_h, x_a and $\dot{x}_a$, which yield muscle contractile element force F_h as a function of time.
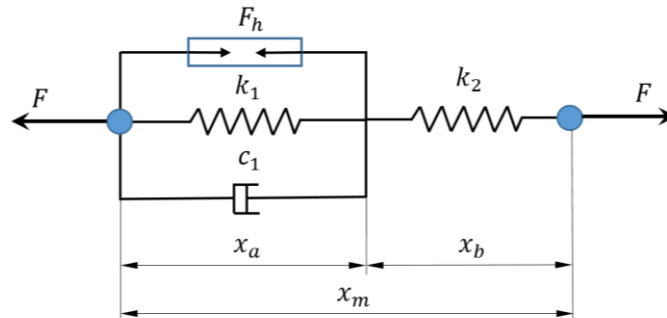
**Fig 2.** The Hill-type muscle model

3. Running Gait Planning

There are two approaches of using forward dynamics or inverse dynamics for gait planning. In the first approach, an optimization problem with respect to initial condition of the robot and actuator force profiles is solved to obtain a periodic gait satisfying the constraints. In this research, the second approach is used because the system is fully actuated. This approach first considers a desired trajectory for the robot and then utilizes inverse dynamics to calculate the amount of muscle force needed to generate the desired gait. Then, a muscle model is used to calculate the actuation force of the muscle's contractile element.

3.1. Stance Phase

We use a point mass biped (PMB) model that has a massless force-actuated leg as the template for the real robot, and we consider a degree-4 polynomial trajectory for it in the stance phase, as shown in Fig. 3. The leg force is denoted by F_r and the leg angle, with respect to vertical, by θ. The degree-4 polynomial path is similar qualitatively to the SLIP trajectory and can generate running gaits with any desired initial condition of the stance phase with the correct initial and final accelerations [9]. The PMB path in the stance phase is considered as

$$y = a_2 x^4 + a_1 x^2 + a_0, \tag{6}$$

in which coefficients a_i are calculated using the COM initial position, velocity, and acceleration. Combining the path equation with the dynamic equation of the PMB system leads to a second order nonlinear differential equation [9]. By solving this equation numerically, the trajectory is calculated as a function of time.
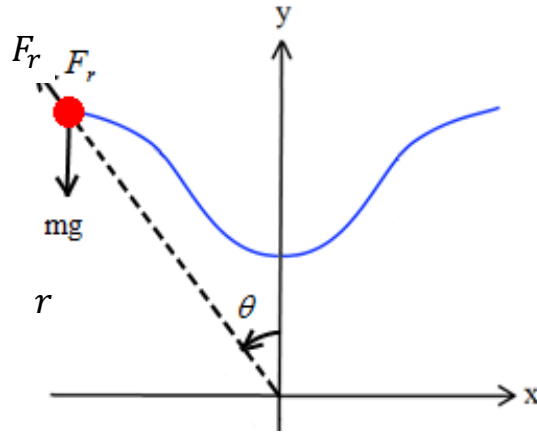
Fig 3. The degree-4 polynomial trajectory of the robot COM in the stance phase

Knowing the COM trajectory of the multibody robot, we need to convert it to the links' motions. In the stance phase, the stance leg and swing leg move separately. Stance leg angles θ_1 and θ_2 are calculated using the position of the fixed pivot A and hip joint E in each instance (Fig. 4a). Because the torso angle is assumed to be fixed and the legs' masses are negligible relative to the torso, we assume the robot mass is concentrated in point E. So, the trajectory of point E is the planned degree-4 polynomial (6). The swing leg angles are inspired by professional runner Usain Bolt's running gait, which is shown in Fig. 5. He is the fastest man in the world as of 2019, holding several Olympic records in running. According to the video frames, he flexes his swing knee to decrease the moment of inertia of the swing leg as much as possible. This increases the swing leg angular velocity without the need of muscle forces by the law of angular momentum conservation. So, we consider the desired angle between the thigh and shin of the swing leg to be constant, θ_{knee}, during the stance phase. The swing leg angle (from hip to toe) is assumed to be symmetric with the stance leg, as shown in Fig. 4b. The relative velocity relationship between the two ends of each joint, for example

$$\vec{v}_C = \vec{v}_A + \vec{\omega}_{AC} \times \vec{r}_{C/A},$$

(a)   (b)
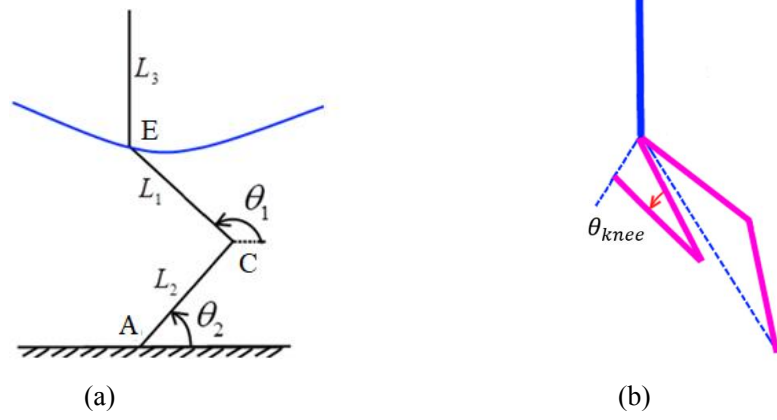
Fig 4. Planning leg angles in stance phase (a) stance leg (b) swing leg

Fig 5. A professional runner's leg angles during the stance phase

and their relative acceleration relationship,

$$\vec{a}_C = \vec{a}_A + \vec{\omega}_{AC} \times (\vec{\omega}_{AC} \times \vec{r}_{C/A}) + \vec{\alpha}_{AC} \times \vec{r}_{C/A},$$

are solved together to find the angular velocity and acceleration of each link.

Muscle forces during the stance phase are calculated using inverse dynamics by substituting the angular velocity and acceleration of links into Eq. (1) in each instance.

3.2. Flight Phase

In the flight phase, the robot's COM moves as a projectile, but its links need to be controlled to touch down with an appropriate condition. To plan the trajectory of the robot links in the flight phase, a degree-5 polynomial versus time, Eq. (7), is considered for each link because it is sufficient to capture the initial and final velocities and accelerations.

$$\theta(t) = a_1 t^5 + a_2 t^4 + a_3 t^3 + a_4 t^2 + a_5 t + a_6 \tag{7}$$

In this equation, coefficients a_1 to a_6 are obtained using the desired angle, angular velocity, and angular acceleration of each link at the take-off and pre-touch-down moments. The time duration of the flight phase is derived using the PMB model. The angular velocity and acceleration of the links as a function of time are obtained using time

derivatives of Eq. (7). Then, the muscles forces are calculated using inverse dynamics (2).

3.3. Energy Expenditure Function

To measure the energy expenditure of the robot, we use the cost of transport (COT) function that is the consumed energy per unit weight per unit distance traveled.

$$\text{COT} = \frac{W}{(m_1 + m_2 + m_3 + m_4 + m_5)gL},$$

in which L is the step length. W is the mechanical work done during the stance and flight phases, which is calculated for overall muscle as

$$W_F = \sum_{i=1}^{4} \left(\int_0^{t_{stance}} \left| F_i \dot{x}_{m,i} \right| dt + \int_{t_{stance}}^{t_{stance} + t_{flight}} \left| F_i \dot{x}_{m,i} \right| dt \right)$$

and for the muscle contractile element as

$$W_{F_h} = \sum_{i=1}^{4} \left(\int_0^{t_{stance}} \left| F_{h,i} \dot{x}_{a,i} \right| dt + \int_{t_{stance}}^{t_{stance} + t_{flight}} \left| F_{h,i} \dot{x}_{a,i} \right| dt \right). \tag{8}$$

Using these two works, we can calculate overall muscle cost of transport COT_F and contractile element cost of transport COT_{F_h} to investigate muscle efficiency effects.

4. Simulation Results

A COM trajectory as Eq. (6) is planned for the stance phase with an initial leg length of $r = 0.823 \ m$, angle of $\theta = 0.360 \ rad$, initial COM velocity of $\dot{x}_{cm} = 3\frac{m}{s}, \dot{y}_{cm} = -0.5\frac{m}{s}$, and initial COM acceleration of $\ddot{x}_{cm} = 0, \ddot{y}_{cm} = -g$. Since the system (1) is fully actuated, its inverse dynamics can be solved using the method described in Section 3.1 to make the robot's COM undergo trajectory (6). Then, the flight inverse dynamics (2) is solved to make the robot links undergo trajectories (7). These calculations result in required muscle forces $F_1(t), F_2(t), F_3(t)$ and $F_4(t)$ for one complete step of running.

The constants L_{ex}, $\theta_{ex,knee}$, $\theta_{ex,hip}$, and $\theta_{ex,knee}$ (Figs. 1 and 4) that have significant effects on the results are considered as gait planning parameters. To study the effects of these parameters on nonlinear dynamics of the system, we consider discrete values for them within their acceptable range as

$$L_{ex} = 0.1, \ 0.15, \ 0.2 \ m$$
$$\theta_{ex,knee} = 155°, \ 165°, \ 175°$$
$$\theta_{ex,hip} = 155°, \ 165°, \ 175°$$
$$\theta_{knee} = 30°, \ 48°, \ 66°, \ 84°.$$

Gait planning is executed for all combinations of these parameters' values. The maximum force value of all muscles, $F_i, i = 1,2,3,4$, during one step in each case is shown in Fig. 6. In this figure, the horizontal axis shows θ_{knee}, subplots of each row has a constant $\theta_{ex,knee}$, and each column has a constant $\theta_{ex,hip}$. The numbers written in each

curve show its L_{ex} value. F_{max} decreases with increasing θ_{knee}, decreases with L_{ex}, decreases with $\theta_{ex,knee}$, and increases with $\theta_{ex,hip}$. Therefore, to restrict the maximum force of the muscles, we need to choose larger θ_{knee}, greater L_{ex}, larger $\theta_{ex,knee}$, and smaller $\theta_{ex,hip}$. However, the bone extension length L_{ex} would be restricted by the robot geometrics.

In each simulated case, we calculate the overall muscle COT. Interestingly, COT_F is only a function of θ_{knee}, as shown in Fig. 7, and is constant while the other three parameters vary. This is because, although changing the bone extension length and angle varies the muscles force and velocity profiles, the time integral of their product is constant for a specific trajectory of the robot. Therefore, to have a smaller COT, we have to choose a larger θ_{knee} of the swing leg in the stance phase.

We use a Hill-type muscle model to calculate the contractile elements' force profiles and their COT. The parameters of Hill-type muscles are chosen to have proper values for the robot mass and geometrics, as shown in Table 1. With this actuating system, COT_{F_h} is calculated using Eq. (8) for each running gait simulation. The plots in Fig. 8 show that COT_{F_h} decreases with θ_{knee}, L_{ex}, and $\theta_{ex,knee}$, and increases with $\theta_{ex,hip}$. Theses trends are similar to the trends of F_{max}.
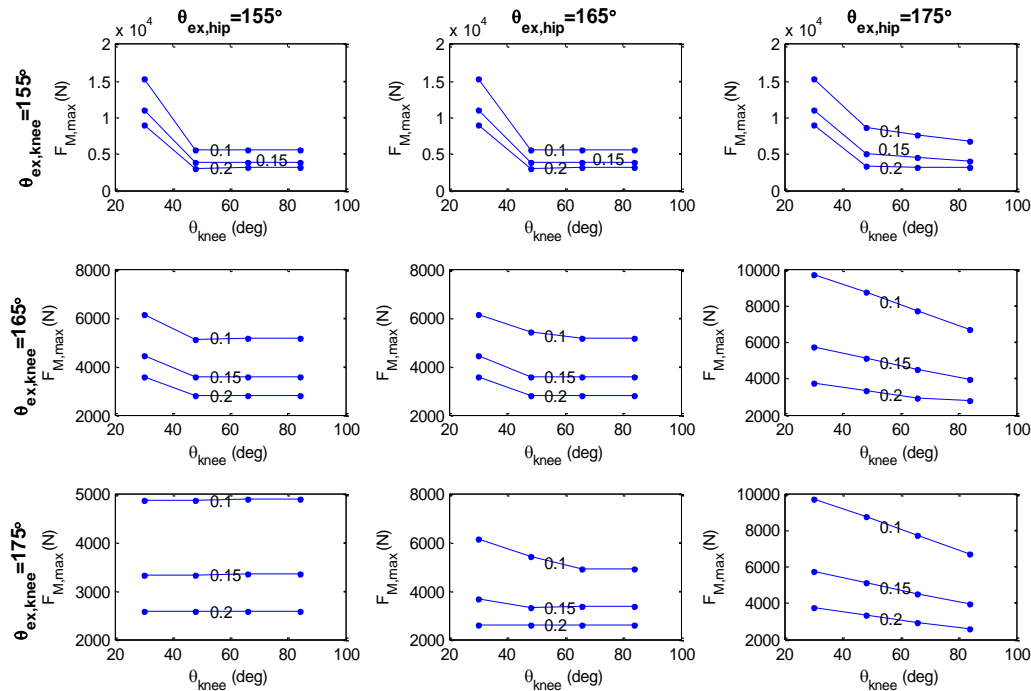
**Fig 6.** Max muscle force variations with respect to gait parameters
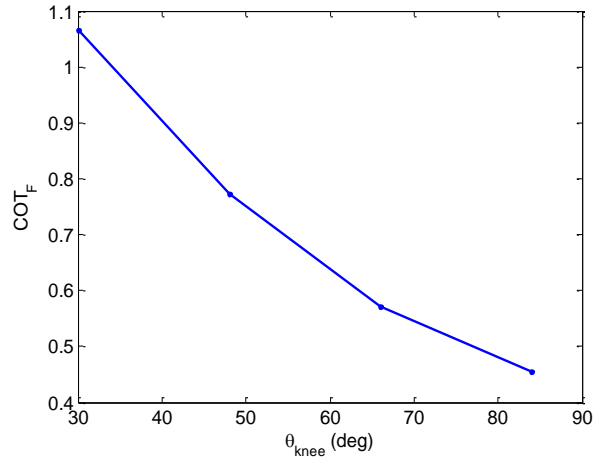
Fig 7. Variations of COT_F with respect to the swing knee angle

Minimizing the 4-dimensional linear interpolation of the data leads to the minimum point of the discrete nodes, and the spline or cubic interpolation leads to some internal points that, due to nonlinearities of the problem, do not generate a minimal COT gait. Therefore, to find the optimal gait parameters, we take the discrete parameters point that minimizes COT_{F_h}, satisfying the geometric constraints. These optimal parameters are $\theta_{knee} = 84°$, $L_{ex} = 0.15m$, $\theta_{ex,knee} = 175°$, and $\theta_{ex,hip} = 155°$.

**Table 1-** Hill-type muscle parameters of the robot actuating system

| Parameter	Value
k_1	$1\ kN/m$
k_2	$30\ kN/m$
c_1	$10\ Ns/m$
Free length of x_1	$0.25\ m$
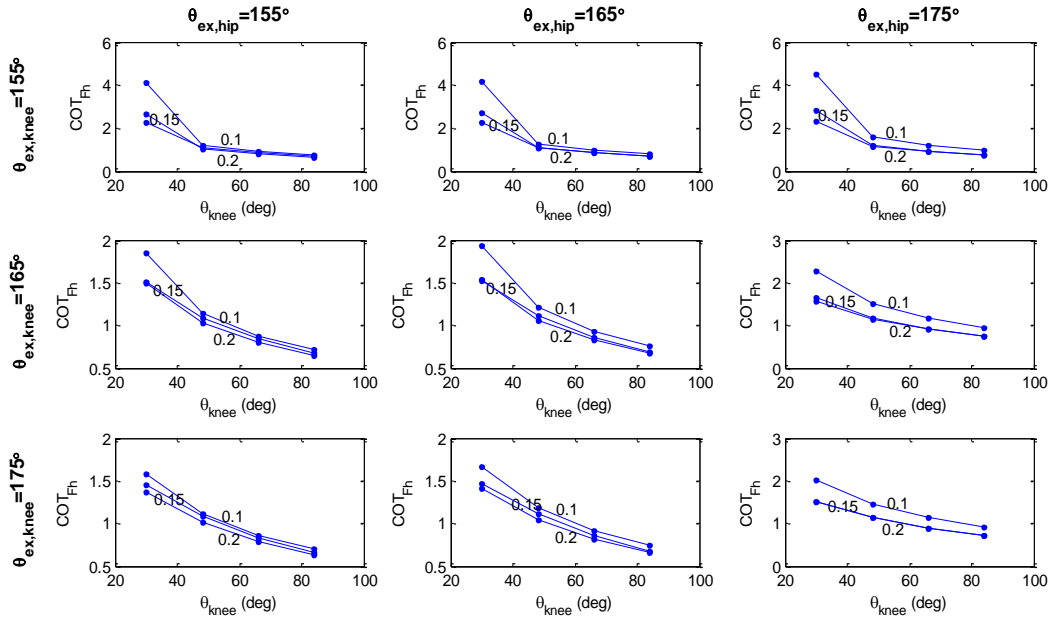
Fig 8. Variations of COT_{F_h} ions with respect to gait parameters

The stick diagram of the simulated optimum gait is shown in Fig. 9. The generated COM path of the robot in the stance phase is depicted by a curve, the planned degree-4 polynomial (6). The swing leg angle is kept constant in the stance phase and varies to the desired value of the next step during the flight phase.

For the optimum gait, the muscles' external forces are calculated using inverse dynamics in each phase; their diagrams are shown in Fig. 10. In this figure, the dashed lines depict flight phase forces. These force profiles are the needed control inputs for the 5-link robot, in which muscles have been replaced with force actuators. The knee force of the stance leg (F_1) has the biggest amount $(-3341\ N)$ in the stance phase because it bears the robot's weight. The hip forces (F_2, F_3) have larger peaks in the flight phase because they need to move the legs to the desired state before touch-down with relatively large accelerations.
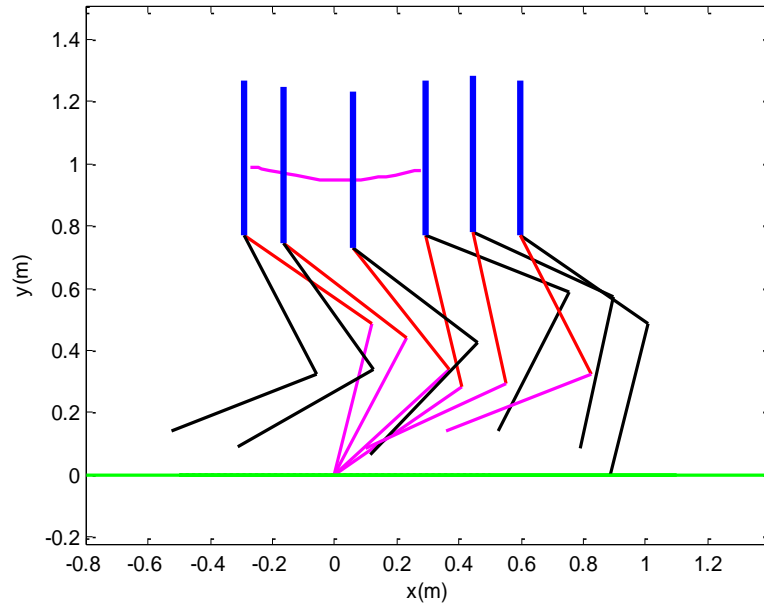
**Fig 9.** Stick diagram of the planned running gait
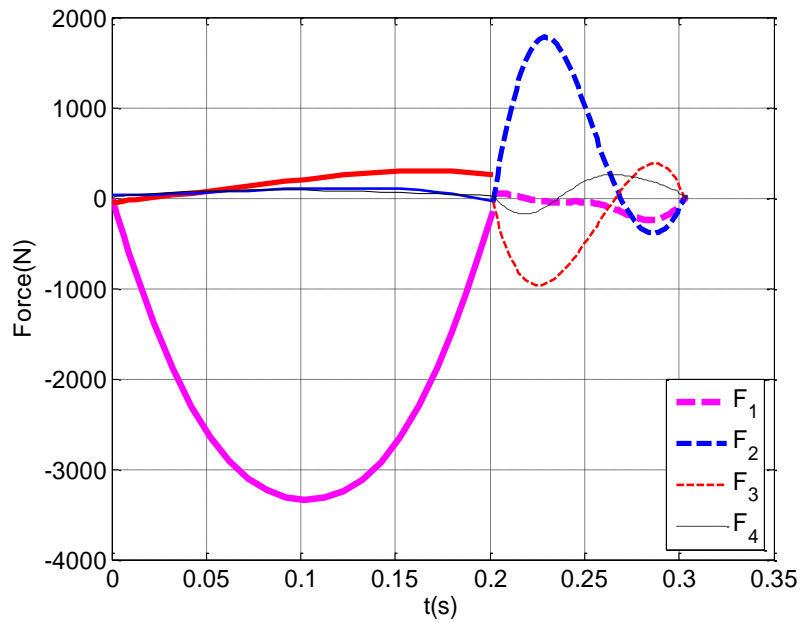
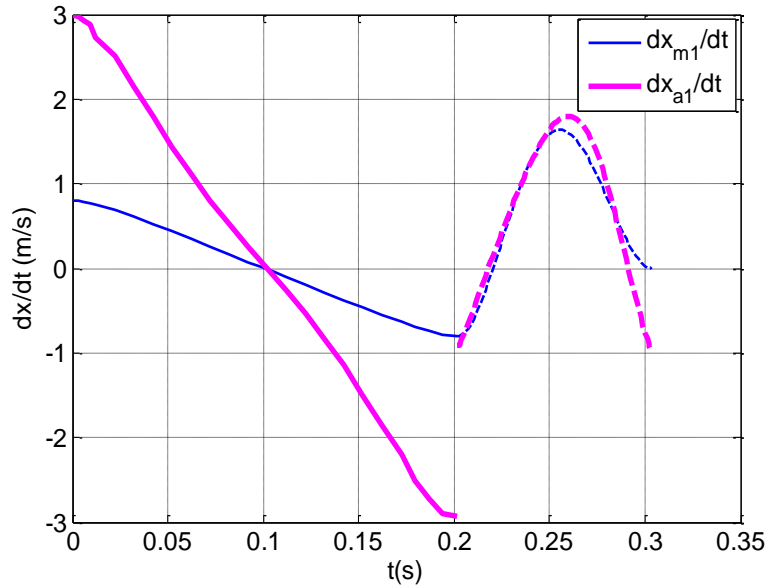**Fig 10.** Muscles' external forces for the running gait

Knowing the force profile of each muscle end, we calculate its contractile element force. The resulted forces F_h have profiles similar to Fig. 10 with small differences. Figure 11 shows the muscle ends and the muscle contractile

element force profiles of muscle 1. Solid lines are for the stance phase, and dashed lines are for the flight phase. The maximum amount of force for this muscle is -3478 N, which is 4% greater than the muscle's external force.

This gait has an overall muscle cost of transport of $COT_F = 0.46$ and a contractile element cost of transport of $COT_{F_h} = 1.45$, which has been increased considerably by using the muscle. This result can be justified using the muscle's external and contractile element velocity profiles shown in Fig. 12. In the first half of the stance phase, the muscle elongates (positive velocity), and, it contracts in the second half (negative velocity). In both cases, the contractile element has larger velocities that increase its consumed power and COT. Therefore, using a single Hill-type actuation system for a biped running robot has negative effects on both the maximum actuating force and COT. Its advantage is to isolate the external impacts from the contractile element.
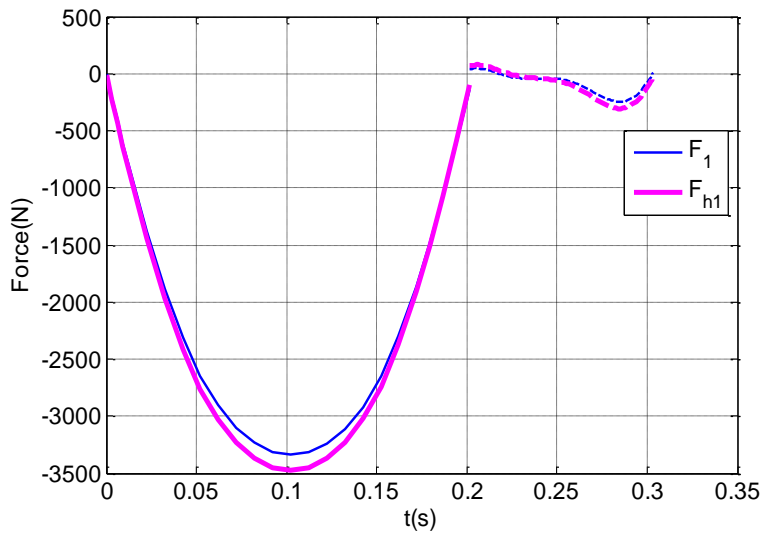
Fig 11. Muscle 1's external and contractile element force profiles for the running gait

Fig 12. Muscle 1's external and contractile element velocity profiles for the running gait

The COT of the biped model's running gait with and without muscles compared to other references are shown in Table 2. Our planned biped running gait without muscles has a good COT compared to other multibody biped robot gaits. The COT with muscles is acceptable compared to the real robots, which is the optimum COT value for the actuation system assumed in this paper. However, it can be improved by searching other actuation system structures for Hill-type muscle actuators like bi-articular muscles.

Table 2- Cost of Transport of different biped models

Biped System	COT (J/Nm)	Reference
Human	0.28	[17]
Monopod I	0.7	[13]
Monopod II	0.22	[13]
HRP-2L	3.57	[14]
Optimized gait for a biped model	1.02	[10]
Parallel Elastic actuating model	1.31	[16]
PMB model with degree 4 polynomial path	0.24	This work
The 5 link biped without muscles	0.46	This work
The 5 link biped with muscles	1.45	This work

5. Conclusions

In this work, a 5-link biped robot model with a Hill-type muscle actuation system was proposed to study the Hill-type muscle effects on biped running efficiency. A dynamic model of the multibody biped model with a muscle-like actuation system was presented. A COM trajectory with a desired initial position and velocity was planned, and the robot's muscle force and velocity profiles were calculated to make the robot undergo the desired trajectory. Then, the force and velocity profiles of the muscle's contractile elements were found using a muscle model, and its COT was calculated. In addition, the effects of the geometric model parameters on COT and F_{max} was investigated.

Unexpectedly, utilizing a single Hill-type muscle for each joint caused an increase in both the COT and F_{max} for the biped mechanism assumed in this work. This is because, when the Hill-type muscle contracts or extracts actively, both the series elastic element and parallel elastic element oppose the contractile element and increase its required force. Also, when the contractile element contracts, the series elastic element is stretched, which increases the contractile element contraction velocity relative to the muscle end's velocity. Optimizing muscle stiffness parameters to minimize COT_{F_h} and F_{max} yields to zero stiffness of the parallel spring and infinite stiffness of the series spring that means substitution of the Hill-type muscle with a single force actuator. Therefore, using a single Hill-type muscle actuation system in each joint with the proposed structure in this paper is not beneficial for robotic energetics and benefits only impact isolation and motor protection.

In future works, the effects on overall motion energetics of the arrangement of a single muscle, bi-articular muscles, and pre-stretched muscles will be studied. In a bi-articular structure, muscles can generate only active tension, and the parameters of its pair muscle's passive tension can be investigated.

REFERENCES

[1] *Hill A.* The abrupt transition from rest to activity in muscle // Proceedings of the Royal Society of London. Series B-Biological Sciences, 1949. - vol. 136, pp. 399-420.

[2] *Lichtwark G. A., Bougoulias K., Wilson A.* Muscle fascicle and series elastic element length changes along the length of the human gastrocnemius during walking and running // Journal of biomechanics – 2007. - vol. 40, pp. 157-164.

[3] *Iida F., Rummel J., Seyfarth A.* Bipedal walking and running with spring-like biarticular muscles, Journal of biomechanics, 2008. - vol. 41, pp. 656-667.

[4] *Hosoda K., Takuma T., Nakamoto A., Hayashi S.* Biped robot design powered by antagonistic pneumatic actuators for multi-modal locomotion // Robotics and Autonomous Systems, 2008. - vol. 56, pp. 46-53.

[5] *Niiyama R., Nishikawa S., Kuniyoshi Y.* Athlete robot with applied human muscle activation patterns for bipedal running // 10th IEEE-RAS International Conference on Humanoid Robots (Humanoids), 2010. - pp. 498-503.

[6] *Geyer H., Seyfarth A., Blickhan R.* Compliant leg behavior explains basic dynamics of walking and running // Proceedings of the Royal Society B, 2006. - 273:2861-2867.

[7] *Srinivasan M., Ruina A.* Computer optimization of a minimal biped model discovers walking and running // Nature, 2006. - Vol 439, pp. 72-75, doi: 10.1038/nature04113.

[8] *Rebula J.R., and Kuo A.D.* The Cost of Leg Forces in Bipedal Locomotion: A Simple Optimization Study // PloS ONE, 2015. - 10.2.

[9] *Dadashzadeh B., Esmaeili M., Macnab C.* Arbitrary Symmetric Running Gait Generation for an Underactuated Biped Model // PloS ONE, 2017. - pp. 0170122, doi: 10.1371.

[10] *Guo Q., Macnab C., Pieper J. K.* Generating efficient rigid biped running gaits with calculated take-off velocities // Robotica, 2011. - vol. 29, pp. 627-640.

[11] *Poulakakis I., Grizzle J.W.* The Spring Loaded Inverted Pendulum as the Hybrid Zero Dynamics of an Asymmetric Hopper // IEEE Transactions on Automatic Control, 2009. - vol. 54, no. 8, pp. 1779-1793.

[12] *Dadashzadeh B., Vejdani H.R., Hurst J.* From Template to Anchor: A Novel Control Strategy for Spring-Mass Running of Bipedal Robots // IEEE/RSJ International Conference on Intelligent Robots and Systems (IROS), Chicago, Illinois, September 2014. - pp. 2566-2571, 978-1-4799-6933-3/14.

[13] *Ahmadi M., Buehler M.* The ARL monopod II running robot: Control and energetics // Proceedings of IEEE International Conference on Robotics and Automation, 1999. - pp. 1689-1694.

[14] *Nagasaki T., Kajita S., Yokoi K., Kaneko K., Tanie K.* Running pattern generation and its evaluation using a realistic humanoid model // Proceedings of IEEE International Conference on Robotics and Automation, 2003. - pp. 1336-1342.

[15] *Grizzle J.W., Hurst J., Morris B., Park H.W., Sreenath K.* MABEL, a new robotic bipedal walker and runner // In Proc. Conf. on American Control Conference ACC'09, 2009.

[16] *Dadashzadeh B., Mahjoob M.J., Nikkhah Bahrami M., Macnab C.* Compliant leg architectures and a linear control strategy for the stable running of planar biped robots // International Journal of Advanced Robotic Systems, 2013. - vol. 10, p. 320.

[17] *Roberts R.K.T., Weyand P., Taylo R.* Energetics of bipedal running, Part I. Metabolic cost of generating force // J. Exp. Bio., 1998. - vol. 201, pp. 2745–2751,.

[18] *Morris B., Grizzle J.* Hybrid invariance in bipedal robots with series compliant actuators // 45th IEEE Conference on Decision and Control, 2006. - pp. 4793-4800.